

***Ab initio* theory of temperature dependence of magnetic anisotropy in layered systems: Applications to thin Co films on Cu(100)**

Á. Buruzs and P. Weinberger

Center of Computational Materials Science, Technical University Vienna, A-1040 Gumpendorferstrasse 1.a., Vienna, Austria

L. Szunyogh and L. Udvardi

Center of Computational Materials Science, Technical University Vienna, A-1040 Gumpendorferstrasse 1.a., Vienna, Austria and Department of Theoretical Physics, Budapest University of Technology and Economics, Budafoki u. 8., H-1111 Budapest, Hungary

P. I. Chleboun, A. M. Fischer, and J. B. Staunton

Department of Physics, University of Warwick, Coventry CV4 7AL, United Kingdom

(Received 2 November 2006; revised manuscript received 15 May 2007; published 14 August 2007)

In this paper we present an extension of the relativistic disordered local moments (RDLM) scheme to layered systems in order to perform *ab initio* calculations of the temperature-dependent magnetic anisotropy energy of magnetic surfaces, interfaces, or films. As implemented within the relativistic spin-polarized screened Korringa-Kohn-Rostoker method, we apply this scheme to thin $\text{Co}_n/\text{Cu}(100)$ films and observe a temperature dependence of the magnetic anisotropy energy (MAE) that significantly differs from that of the bulk systems studied so far. In addition to the overall agreement of our results with experiments in showing an in-plane magnetization for almost all layer thicknesses and temperatures under consideration, our calculations also systematically predict a temperature-induced reverse (in-plane to out-of-plane) spin reorientation. In order to explain this unexpected feature we fit the parameters of a classical Heisenberg model solved within the mean-field approach to the MAE obtained from the RDLM calculations, and conclude that the spin reorientation is driven by a competition of exchange and single-site anisotropies.

DOI: [10.1103/PhysRevB.76.064417](https://doi.org/10.1103/PhysRevB.76.064417)

PACS number(s): 75.70.Ak, 75.30.Gw, 75.50.Ss

I. INTRODUCTION

The developments made in recent decades in the field of high-density magnetic data storage created significant interest in the magnetocrystalline anisotropy (MCA) of magnetic thin films. The writing process on a magnetic storage medium is performed by applying a magnetic field, the required magnitude of which is governed by the magnetic anisotropy (K), i.e., the energy difference between different possible magnetization directions. For the sake of easier writing, the sample is heated, because then the magnetic anisotropy decreases with increasing temperature. In order to understand this process and design new magnetic storage devices, it is therefore necessary to investigate also the temperature dependence of the magnetic properties.

The first significant theoretical study concerning the temperature-dependent MCA was already published at the end of the 1960s.¹ In this study a single-ion anisotropy model was assumed, and implicit analytical formulas were deduced for the temperature and magnetization dependence of the anisotropy constants. From the late 1990s on, also analytical Green function methods were applied to describe the temperature dependence of the MCA.² In these methods appropriate decoupling procedures^{2,3} are used to take into account thermal fluctuations and collective excitations beyond the mean-field description. Recently even *ab initio* methods have been applied to investigate the MCA.^{4,5} Mryasov *et al.*⁴ set up a model Hamiltonian based on constrained local density approximation calculations and included the temperature dependence by performing Langevin dynamics simulations with this Hamiltonian. They get a $K(T) \sim M^{2.1}(T)$ relation for

the anisotropy energy versus magnetization dependence for $L1_0$ FePt.

Other works^{5,6} are based on the disordered local moment (DLM) scheme.⁷ The DLM is based on the idea that in itinerant metallic magnets, on a certain time scale τ , which is small as compared to the characteristic time of spin fluctuations, but longer than the electron hopping times, the spin orientations of the electrons leaving an atomic site are sufficiently correlated with those arriving such that a nonzero magnetization exists when the appropriate quantity is averaged over τ . In the DLM scheme the magnetic excitations are modeled by associating local spin-polarization axes with all lattice sites and the orientations $\{\hat{e}\}$ vary very slowly on the time scale of the electronic motions. These local moment degrees of freedom produce local magnetic fields centered at the lattice sites, which in turn affect the electronic motions and are self-consistently maintained by them. By taking appropriate ensemble averages over the orientational configurations, the system's magnetic properties can be determined. In the first applications of the DLM approach, paramagnetic electron systems could be described by formally mapping "up" and "down" moments onto the problem of a disordered binary alloy $A_{0.5}B_{0.5}$ with A and B representing the constituents. To compute the configuration average the well-tryed Korringa-Kohn-Rostoker (KKR) coherent potential approximation (CPA) was used. From the temperature-dependent paramagnetic susceptibility⁸ the Curie temperature was determined even for thin films.⁹

Recently, we developed a DLM scheme in order to take into account every local moment direction weighted with a statistical probability, such that investigations below the Cu-

rie temperature are accessible. The MCA is caused largely by spin-orbit coupling, so a relativistic treatment is necessary. Staunton *et al.*⁵ investigated the MCA of bulk $L1_0$ -ordered FePt, $L1_0$ FePd, and Fe₅₀Pt₅₀ solid solutions⁶ and found deviations from the Callen-Callen single-ion anisotropy rule. For the uniaxial magnets $L1_0$ FePt and FePd they obtained a $K(T) \sim M^2(T)$ anisotropy-magnetization dependence and for the cubic magnet Fe₅₀Pt₅₀ $K(T) \sim M^6$, in good agreement with experiment. In the present paper we extend this theory to layered systems and apply it to ferromagnetic Co films deposited on a Cu(001) surface.

II. THE RELATIVISTIC DLM METHOD FOR LAYERED SYSTEMS

The theory of disordered local moments in conjunction with the Korringa-Kohn-Rostoker coherent potential approximation was proposed more than 20 years ago by Györffy *et al.*⁷ and has recently been generalized by Staunton *et al.*^{5,6} to include relativistic effects. In this section we briefly outline how to use this scheme for layered systems, i.e., for systems with two-dimensional translation invariance and introduce a few new concepts concerning the calculation of Weiss fields and the MCA energy.

The key quantity of the DLM scheme is the electronic grand potential $\Omega^{(\hat{n})}(\{\hat{\epsilon}\})$ of a ferromagnetic system as obtained within the local spin-density approximation (LSDA) for a given direction of the magnetization, \hat{n} , as a function of the orientations of the local spins, $\{\hat{\epsilon}\}$. The DLM method is therefore not confined to a model Hamiltonian with a fixed form such as a classical Heisenberg model, but, at least within the LSDA, takes into account spin-spin correlations to any order.

In the case of a layered system, i.e., for a system with 2D translational invariance and, for brevity, with one sublattice per geometrical layer the Weiss field in a given layer p , $\tilde{h}_p^{(\hat{n})} = h_p^{(\hat{n})} \hat{n}$ is defined by⁶

$$h_p^{(\hat{n})} = \frac{3}{4\pi} \int d\hat{\epsilon}_{pi} (\hat{\epsilon}_{pi} \cdot \hat{n}) \langle \Omega^{(\hat{n})} \rangle_{\hat{\epsilon}_{pi}} \quad (1)$$

where $\langle \Omega^{(\hat{n})} \rangle_{\hat{\epsilon}_{pi}}$ denotes a thermodynamical average over the orientations of the spins at all sites in the system with the exception of a particular site i in layer p , for which $\hat{\epsilon}_{pi} = (\sin \vartheta_{pi} \cos \varphi_{pi}, \sin \vartheta_{pi} \sin \varphi_{pi}, \cos \vartheta_{pi})$. The layer-resolved probabilities

$$P_p^{(\hat{n})}(\hat{\epsilon}_{pi}) = \frac{\beta h_p^{(\hat{n})}}{4\pi \sinh(\beta h_p^{(\hat{n})})} \exp[-\beta h_p^{(\hat{n})}(\hat{\epsilon}_{pi} \cdot \hat{n})], \quad (2)$$

where $\beta = 1/k_B T$, are then used to solve the conditions of the coherent-potential approximation for the effective medium described within the Korringa-Kohn-Rostoker method in terms of layer-resolved scattering t matrices $\underline{t}_p^{c(\hat{n})}$ and the scattering path operator matrix $\underline{\tau}^{c(\hat{n})} = \{\underline{\tau}_{pi,pj}^{c(\hat{n})}\}$ (underlined symbols refer to matrices in angular momentum space).

In the spirit of the magnetic force theorem,¹¹ the free energy is approximated by the single-particle grand potential (band energy),

$$\Omega^{(\hat{n})}(\{\hat{\epsilon}\}) \simeq - \int d\epsilon f(\epsilon; \mu) N^{(\hat{n})}(\epsilon; \{\hat{\epsilon}\}), \quad (3)$$

where μ is the chemical potential, $f(\epsilon; \mu)$ is the Fermi-Dirac distribution, and $N^{(\hat{n})}(\epsilon; \{\hat{\epsilon}\})$ denotes the integrated density of states, which can be expressed in terms of Lloyd's formula.¹² The Weiss field can then be calculated as

$$h_p^{(\hat{n})} = \frac{3}{4\pi^2} \text{Im} \int d\epsilon f(\epsilon; \mu) \times \left(\int d\hat{\epsilon}_{pi} (\hat{\epsilon}_{pi} \cdot \hat{n}) \ln \det \underline{M}_p^{(\hat{n})}(\epsilon; \hat{\epsilon}_{pi}) \right), \quad (4)$$

where

$$\underline{M}_p^{(\hat{n})}(\epsilon; \hat{\epsilon}_{pi}) = \underline{1} + [\underline{t}_p(\epsilon; \hat{\epsilon}_{pi})^{-1} - \underline{t}_p^{c(\hat{n})}(\epsilon)^{-1}] \underline{\tau}_{pi,pi}^{c(\hat{n})}(\epsilon). \quad (5)$$

In the case of spherically symmetric effective potentials and fields, $\underline{t}_p(\epsilon; \hat{\epsilon}_{pi})$ can be calculated in terms of the following similarity transformation:

$$\underline{t}_p(\epsilon; \hat{\epsilon}_{pi}) = \underline{R}(\hat{\epsilon}_{pi}) \underline{t}_p(\epsilon; \hat{z}) \underline{R}(\hat{\epsilon}_{pi})^+, \quad (6)$$

where $\underline{t}_p(\epsilon; \hat{z})$ refers to the case of an effective field pointing along the z axis and $\underline{R}(\hat{\epsilon}_{pi})$ contains blockwise the projective representations of the $O(3)$ transformation that rotates the z axis into $\hat{\epsilon}_{pi}$.

We developed an approximate but less demanding way of calculating the Weiss fields. In supposing an orientational dependence for the restricted grand potential,

$$\langle \Omega^{(\hat{n})} \rangle_{\hat{\epsilon}_{pi}} = \Omega^{c(\hat{n})} + h_p^{(\hat{n})}(\hat{\epsilon}_{pi} \cdot \hat{n}) + K_p \sin^2 \vartheta_{pi}, \quad (7)$$

where $\Omega^{c(\hat{n})}$ is the grand canonical potential of the completely disordered effective medium and K_p is a microscopic uniaxial anisotropy constant, the Weiss field can be obtained from the derivative of $\langle \Omega^{(\hat{n})} \rangle_{\hat{\epsilon}_{pi}}$ with respect to the average magnetization direction \hat{n} . The result for $\hat{n} = \hat{z}$ is given by

$$h_p^{(\hat{z})} = - \frac{1}{\pi} \text{Im} \int d\epsilon f(\epsilon; \mu) \times \text{Tr} \left(\frac{\partial \underline{t}_p(\epsilon; \hat{\epsilon}_{pi})^{-1}}{\partial \vartheta_{pi}} \underline{\tau}_{pi,pi}^{c(\hat{z})}(\epsilon) \underline{D}_p^{(\hat{z})}(\epsilon; \hat{\epsilon}_{pi}) \right)_{\hat{\epsilon}_{pi} = \hat{z}}, \quad (8)$$

with $\underline{D}_p^{(\hat{z})}(\epsilon; \hat{\epsilon}_{pi}) \equiv \underline{M}_p^{(\hat{z})}(\epsilon; \hat{\epsilon}_{pi})^{-1}$. Similar expressions can be obtained for any direction \hat{n} of the Weiss fields. Reassuringly enough, the above two methods, Eqs. (4) and (8), gave the same result for the Weiss fields within about 1% numerical accuracy. The average magnetization in layer p can then be calculated as

$$m_p^{(\hat{n})} = \int d\hat{\epsilon}_{pi} (\hat{\epsilon}_{pi} \cdot \hat{n}) P_p^{(\hat{n})}(\hat{\epsilon}_{pi}) = L(-\beta h_p^{(\hat{n})}), \quad (9)$$

with $L(x)$ being the Langevin function.

As in Ref. 6 for calculating the MCA energy we used the torque method.¹³ Assuming for uniaxial systems the following orientational dependence of the free energy:

$$F(\vartheta) = F_0 + K \sin^2 \vartheta, \quad (10)$$

yields for the torque

$$T\left(\vartheta = \frac{\pi}{4}\right) = \frac{dF(\vartheta)}{d\vartheta} \Big|_{\vartheta=\pi/4} = \frac{d\langle\Omega^{(\hat{n})}\rangle}{d\vartheta} \Big|_{\vartheta=\pi/4} = K. \quad (11)$$

In the above formula we replaced the derivative of the free energy with respect to the magnetization angle by the corresponding derivative of the grand potential, which follows from an approximation of neglecting the dependence of $h_p^{(\hat{n})}$ on \hat{n} , implying that the spin-entropy term in the free energy is also independent of \hat{n} .⁶ Note that for $K > 0$ (< 0) the system is magnetized normal (parallel) to the planes. By employing again the magnetic force theorem the LSDA contribution to the magnetic anisotropy constant, usually termed the band energy part K_b , can be given as a sum of layer-resolved contributions $K_{b,p}$,

$$K_b = \sum_p K_{b,p}, \quad (12)$$

where

$$K_{b,p} = \frac{1}{\pi} \text{Im} \int d\varepsilon f(\varepsilon; \mu) \int d\hat{e}_{pi} P_p^{(z)}(\hat{e}_{pi}) \times \text{Tr} \left[\left(\frac{\partial \underline{R}(\hat{n})}{\partial \vartheta} \underline{t}_p(\varepsilon; \hat{e}_{pi})^{-1} \underline{R}(\hat{n})^+ + \underline{R}(\hat{n}) \underline{t}_p(\varepsilon; \hat{e}_{pi})^{-1} \frac{\partial \underline{R}^+(\hat{n})}{\partial \vartheta} \right) \underline{t}_{pi}^{c(\hat{n})}(\varepsilon) \underline{D}_p^{(\hat{n})}(\varepsilon; \hat{e}_{pi}) \right]_{\vartheta=\pi/4, \varphi=0}. \quad (13)$$

Note that for an accurate calculation of $K_{b,p}$ in terms of Eq. (13) the CPA condition, Eq. (29) of Ref. 6, has to be satisfied with a high precision.

The total magnetic anisotropy energy (MAE) also contains a contribution arising from the magnetic dipole-dipole energy (K_{dd}), which we approximate by simply inserting the averaged magnetic moments $M_p(T) = M_p(0)m_p(T)$ (in units of Bohr magnetons) [see also Eq. (9)] into the expression derived for completely ordered ($T=0$ K) ferromagnetic layered systems,

$$E_{dd}^{(\hat{n})} = \sum_{pq} \frac{M_p M_q}{c^2} \hat{n} D_{pq}^{dd} \hat{n}, \quad (14)$$

where c ($=274.072$) is the velocity of light in atomic (Rydberg) units and D_{pq}^{dd} are the dipole-dipole Madelung matrices.¹⁴ The corresponding contribution to the uniaxial MAE is then defined as

$$K_{dd} = E_{dd}^{(\hat{x})} - E_{dd}^{(\hat{z})}. \quad (15)$$

Thus, the total MA constant is given by

$$K = K_b + K_{dd}. \quad (16)$$

III. COMPUTATIONAL DETAILS

The calculations were performed by using the relativistic version of the screened KKR method¹⁰ within the LSDA as parametrized by Vosko *et al.*¹⁵ and the atomic sphere approximation. Self-consistent potentials were calculated both

for the ferromagnetic ground state and for the paramagnetic state; these potentials then were used for the DLM calculations at finite temperatures (see below). The experimental lattice constant of bulk Cu ($a=6.83a_0$) was used, i.e., no attempt was made to include geometrical relaxations in a fcc (001) parent lattice.

For a fixed orientation of the average magnetization \hat{n} and at a given temperature T , our strategy for determining the layer-dependent effective t matrices $t_p^{c(\hat{n})}$ and Weiss fields $h_p^{(\hat{n})}$ simultaneously, is as follows.

(1) Choose an initial (usually uniform) set of $h_p^{(\hat{n})}$.

(2) Solve the CPA condition, with the corresponding probabilities, $P_p^{(\hat{n})}(\hat{e}_{pi})$, Eq. (2). For this step we employed the method proposed by Ginatempo and Staunton,¹⁶ and performed the integral over orientations in terms of a cascade adaptive sampling. This turned out to be numerically very efficient when using a local frame of reference fixed to the average magnetization direction, since in that case $P_p^{(\hat{n})}(\hat{e}_{pi})$ depends just on ϑ_{pi} . The CPA loop was iterated up to a relative accuracy of 10^{-5} for $t_p^{c(\hat{n})}$.

(3) Calculate a new set of $h_p^{(\hat{n})}$ from Eq. (4) or (8). An asymmetric sampling of 16 points on a semicircular contour in the upper complex semiplane was sufficient for the corresponding energy integration to achieve a relative accuracy of 10^{-4} for $h_p^{(\hat{n})}$. In order to keep this accuracy, the Brillouin zone (BZ) integration of the scattering path operator [$t_{pp}^{c(\hat{n})}(\mathbf{k})$] was performed by using a variable k mesh with a maximum of 465 k points in the irreducible (1/8) wedge of the BZ for energies close to the Fermi level.

(4) Repeat steps 2 and 3 until convergence of $h_p^{(\hat{n})}$ is achieved. By using Broyden's second modified method¹⁷ we needed just 5–10 iterations in order to reach the above mentioned accuracy.

After having obtained well-converged Weiss fields and effective t matrices, the band energy part of the MA constant K_b [see Eq. (12)], was calculated using Eq. (13). It turned out, however, that unlike the local moments the MA constant is very sensitive to the self-consistent potentials used. Clearly, a self-consistent calculation of the effective potentials and fields at each temperature would complete the relativistic DLM (RDLM) scheme described above. Here we approximated the potentials in first order of the layer-dependent average magnetizations $m_p(T)$ [see Eq. (9)],

$$V^p(T) = m_p(T)V_{FM}^p + (1 - m_p(T))V_{PM}^p, \quad (17)$$

and similarly for the effective fields, which obviously recovers the limiting cases, i.e., the ferromagnetic ground state of the system is described by the self-consistent potentials and exchange fields V_{FM}^p and B_{FM}^p , while above the Curie temperature the system is in the paramagnetic DLM state, specified by V_{PM}^p and B_{PM}^p , respectively. The parameters for the energy and BZ integrations used for the Weiss fields were sufficient to achieve a relative numerical accuracy of 5% for K_b .

IV. APPLICATION TO Co FILMS ON Cu(001)

Ferromagnetic Co films are known to grow epitaxially on Cu(100) due to the small lattice mismatch, and show a strong

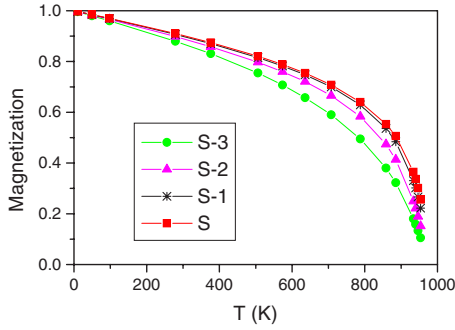


FIG. 1. (Color online) Average magnetizations m_p [see Eq. (9)], versus temperature for $\text{Co}_4/\text{Cu}(100)$. The label S refers to the surface Co layer, $S-n$ ($n=1,2,3$) to the n th Co layer beneath the surface.

in-plane magnetic anisotropy.^{18,19} As this system is experimentally and theoretically well studied it is most suitable for an application of the RDLM scheme for layered systems that we developed. For the present study we performed calculations for film thicknesses of $n=1$ to 6 monolayers.

In Fig. 1 the calculated layer-dependent magnetizations are shown as a function of temperature for the case of the Co_4 film. As can be inferred from this figure the magnetization in all layers vanishes at $T_C=960$ K. Interestingly, however, the shape of the curves differ from layer to layer: the largest overall magnetization corresponds to the surface layer (S), the lowest to the interface layer ($S-3$). This behavior can be attributed to the well-known tendency of enhanced ferromagnetism²⁰ (i.e., enhanced Weiss fields) at the surface due to the reduced coordination of the Co atoms, while at the interface a weakening of the magnetic interactions is expected due to hybridization between electron states of the Co and Cu atoms.

This reasoning can be justified by comparing the DLM results with the mean-field solution of a classical Heisenberg spin model. Supposing isotropic exchange interactions J_{pq} , the mean-field energy takes the simple form

$$E_{MF} = -\frac{1}{2} \sum_{pq} m_p J_{pq} m_q, \quad (18)$$

while the corresponding Weiss fields

$$h_p = \sum_q J_{pq} m_q \quad (19)$$

can be used together with Eq. (9) to determine the average magnetizations m_p as a function of temperature. Figure 2 shows the corresponding results with the parameters $J_{11}=155$ meV, $J_{22}=90$ meV, $J_{33}=70$ meV, $J_{44}=115$ meV, $J_{12}=J_{34}=100$ meV, and $J_{23}=70$ meV (the labels 1, 2 and 3, 4 refer to the surface layer, the intermediate layers, and the layer adjacent to the substrate, respectively). These results reproduce qualitatively well those obtained from the DLM calculations. From this model study, it obviously turned out that the asymmetry of the exchange parameters, in particular, $J_{11} > J_{44}$, and $J_{22} > J_{33}$, is the main source of the asymmetry of the magnetizations, since by choosing $J_{11}=J_{44}$, and $J_{22}=J_{33}$ this asymmetry is completely removed.

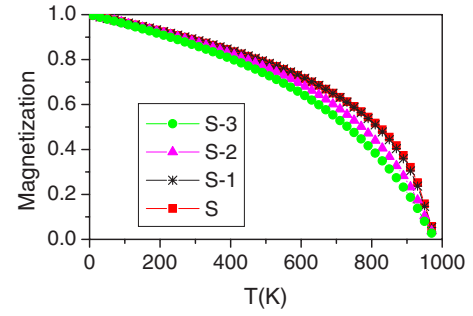


FIG. 2. (Color online) Average magnetizations m_p [see Eq. (9)], versus temperature for $\text{Co}_4/\text{Cu}(100)$ as obtained from a mean-field solution of an isotropic Heisenberg model (see text for the exchange parameters used). The label S refers to the surface Co layer, $S-n$ ($n=1,2,3,4$) to the n th Co layer beneath the surface.

In Table I we summarize the Curie temperatures calculated for different Co layer thicknesses. Reassuringly, these values are consistent with those of Szunyogh and Udvardi²⁰ obtained from a mean-field solution of a Heisenberg model containing exchange parameters as calculated in the paramagnetic DLM state. Razee *et al.*⁹ derived the Curie temperature of $\text{Co}_n/\text{Cu}(100)$ by directly evaluating the spin susceptibility from the paramagnetic DLM state. Although a smaller Curie temperature for the monolayer case was reported, for thicker layers they obtained roughly the same results as here. Experimentally, much smaller Curie temperatures were measured, in particular, for very thin layers, while T_C increased with increasing film thickness according to a power law.^{18,19} The reason for the disagreement with respect to experiment can most probably be attributed to the mean-field approximation used in the *ab initio* DLM theories, which is most critical for very thin layers. In terms of a spin-wave theory and by using estimated bulk parameters for the magnetization and the exchange field, Bruno²¹ obtained about 200 K for T_C of the $\text{Co}_1/\text{Cu}(001)$ system. Pajda *et al.*²² performed first-principles calculations for the exchange parameters J_{ij} in the ferromagnetic ground state of $\text{Co}_1/\text{Cu}(001)$ and showed that by solving the Heisenberg spin model within the random phase approximation reduces the calculated T_C to 426 K with respect to a value of 1043 K predicted by the mean-field theory. Other reasons for the deviation between the experimental and theoretical results can be the incomplete layer growth and surface relaxations in the experimental studies, again most critical for very thin layers. The experimental value of about 950 K for large thicknesses of Co (Ref. 19) is, however, in good agreement with our present (and previous) results. In a recent review²³ Jensen and Bennemann showed that a strong enhancement of the exchange coupling in the surface layer can lead to a considerable deviation from the power scaling law for T_C

TABLE I. Calculated Curie temperatures (K) for $\text{Co}_n/\text{Cu}(100)$.

n	1	2	3	4	5	6
T_C	1330	933	897	960	945	960

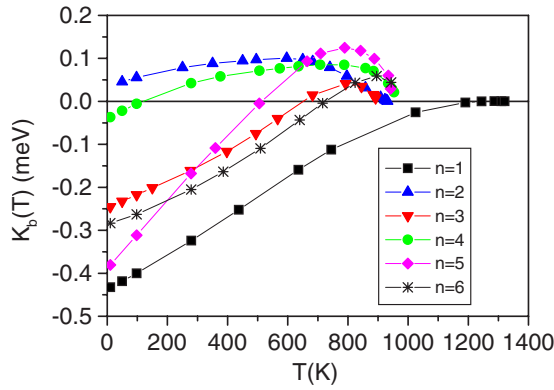


FIG. 3. (Color online) Band energy part of the magnetic anisotropy constant $K_b(T)$ for $\text{Co}_n/\text{Cu}(100)$.

and can result even to an enhancement for very thin magnetic layers. This observation qualitatively explains the trend seen in Table I.

In Fig. 3 the calculated band energy contributions of the magnetic anisotropy energy, K_b , are plotted as a function of temperature. The corresponding values near $T=0$ are consistent with our previous calculations for the ground state in terms of the relativistic screened KKR method showing quite large fluctuations with respect to the layer thickness (see Fig. 1 of Ref. 24). As in the bulk systems studied so far,^{5,6} the MA constant decreases in the monolayer case almost monotonically in magnitude with increasing temperature. For thicker films, however, $K_b(T)$ shows a nonmonotonic temperature behavior with a more or less pronounced maximum. Correspondingly, for the cases of $n \geq 3$, $K_b(T)$ also changes sign at a given temperature. This kind of behavior did not show up in early studies such as in the model description (Ref. 1) or in *ab initio* calculations⁴⁻⁶ of $K_b(T)$.

In order to explain this unusual result, we again used a classical Heisenberg spin model that includes terms arising

from relativistic (spin-orbit coupling) effects to describe magnetic anisotropy. In particular, due to itinerant electrons in a metallic system the anisotropy of the exchange interactions, $J_{pq}^{xx} \neq J_{pq}^{zz}$, has to be accounted for. Similar to the strategy of our *ab initio* RDLM calculations, by taking Eq. (2) with Eq. (19) for the probabilities and supposing orientational independence for the Weiss fields (magnetizations), the anisotropy of the mean-field free energy,

$$K = F^x - F^z = -\frac{1}{2} \sum_{pq} m_p (J_{pq}^{xx} - J_{pq}^{zz}) m_q + \sum_p K_p \left(\frac{3}{\beta h_p} m_p + 1 \right), \quad (20)$$

was then used to fit the exchange anisotropies $\Delta J_{pq} = J_{pq}^{zz} - J_{pq}^{xx}$ and the on-site anisotropies K_p to the $K_b(T)$ values obtained from the RDLM calculations. Note that, in order to reduce the number of fitting parameters, unlike the interpretation of the layer-dependent magnetizations, here we restricted ourselves to exchange parameters that are symmetric with respect to the layers. Indeed, from our tests, we found the moderate asymmetry of the magnetizations (see Fig. 2), to have only a very small effect to the MA constants obtained from the spin model. Furthermore, for some cases we also checked our results by comparing them with a full solution within the mean-field theory,²⁵ i.e., by using the canonical partition function with an exact account of the on-site anisotropies and of the orientational dependence of the magnetizations, and obtained a nearly perfect agreement between the two approaches.

The fitted parameters are listed in Table II, while in Fig. 4 the corresponding magnetic anisotropies, Eq. (20), are shown. As can be seen, the MA constants obtained from the spin model compare qualitatively well with the DLM results, Fig. 3. Inspecting the parameters in Table II it is obvious that the exchange anisotropies ΔJ_{pq} are of the same order of mag-

TABLE II. Model parameters J_{pq} , $\Delta J_{pq} = J_{pq}^{zz} - J_{pq}^{xx}$ and K_p , see Eqs. (19) and (20), fitted to the temperature-dependent MA constants of the $\text{Co}_n/\text{Cu}(100)$ films as obtained from the RDLM calculations. All parameters are given in units of meV.

n	Parameters
1	$J_{11}^c = 336$, $\Delta J_{11} = 0.36$, $K_1 = -0.615$
2	$J_{11}^c = J_{22}^c = 136$, $\Delta J_{11} = 0.36$, $J_{12}^c = 100$, $\Delta J_{12} = 0.64$, $K_1 = -0.37$, $K_2 = -0.615$
3	$J_{11}^c = J_{33}^c = 136$, $\Delta J_{11} = \Delta J_{33} = 0.36$, $J_{22}^c = 60$, $\Delta J_{22} = 0$, $J_{12}^c = J_{23}^c = 100$, $\Delta J_{12} = \Delta J_{23} = 0.4$, $K_1 = -0.37$, $K_2 = -0.425$, $K_3 = -0.615$
4	$J_{11}^c = J_{44}^c = 136$, $\Delta J_{11} = \Delta J_{44} = 0.36$, $J_{22}^c = J_{33}^c = 60$, $\Delta J_{22} = \Delta J_{33} = 0$, $J_{12}^c = J_{34}^c = 100$, $\Delta J_{12} = \Delta J_{34} = 0.23$, $J_{23}^c = 60$, $\Delta J_{23} = 0$, $K_1 = -0.37$, $K_2 = 0$, $K_3 = -0.37$, $K_4 = -0.615$
5	$J_{11}^c = J_{55}^c = 136$, $\Delta J_{11} = \Delta J_{55} = 0.36$, $J_{22}^c = J_{33}^c = J_{44}^c = 60$, $\Delta J_{22} = \Delta J_{33} = \Delta J_{44} = 0$, $J_{12}^c = J_{45}^c = 100$, $\Delta J_{12} = \Delta J_{45} = 0.8$, $J_{23}^c = J_{34}^c = 60$, $\Delta J_{23} = \Delta J_{34} = 0$, $K_1 = -0.37$, $K_2 = -0.37$, $K_3 = -0.37$, $K_4 = -0.615$, $K_5 = -0.615$
6	$J_{11}^c = J_{66}^c = 136$, $\Delta J_{11} = \Delta J_{66} = 0.36$, $J_{22}^c = J_{55}^c = 60$, $\Delta J_{22} = \Delta J_{55} = 0$, $J_{33}^c = J_{44}^c = 20$, $\Delta J_{33} = \Delta J_{44} = 0$, $J_{12}^c = J_{56}^c = 100$, $\Delta J_{12} = \Delta J_{56} = 0.36$, $J_{23}^c = J_{34}^c = J_{45}^c = 60$, $\Delta J_{23} = \Delta J_{34} = \Delta J_{45} = 0$, $K_1 = -0.37$, $K_2 = 0$, $K_3 = 0$, $K_4 = 0$, $K_5 = -0.4$, $K_6 = -0.615$

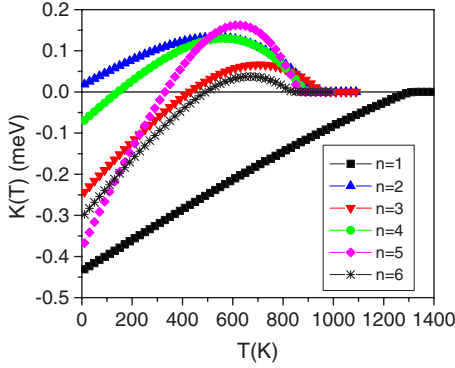


FIG. 4. (Color online) Magnetic anisotropy constants vs temperature obtained from a mean-field approach of the Heisenberg model, Eq. (20), with the fitted parameters listed in Table II.

nitude as the on-site anisotropy energies K_p , but of the opposite sign. Clearly from Eq. (20) the exchange anisotropy part of the MAE is proportional to m^2 , while the on-site anisotropy term follows the Callen-Callen behavior, i.e., $K \propto m^2$ for small m , and $K \propto m^3$ for large m . Thus, an interplay of these two terms in an itinerant electron system can lead to thermal reorientation transition.

In order to demonstrate this effect, we performed model calculations for the MA constants of the $\text{Co}_3/\text{Cu}(100)$ system by uniformly scaling the exchange anisotropies $\Delta J_{pq} = x \Delta J_{pq}^{\text{fit}}$ and the on-site anisotropies $K_p = y K_p^{\text{fit}}$, with $\Delta J_{pq}^{\text{fit}}$ and K_p^{fit} taken from Table II. As a constraint, we kept the MA constant at $T=0$ fixed, from which the scaling factors y can uniquely be determined as a function of x . The corresponding MA constant vs T curves are plotted for selected x values in Fig. 5. As can be seen in this figure, by decreasing the exchange anisotropy the MA constant gradually decreases and the reorientation transition completely disappears below about $x=0.5$. For vanishing exchange anisotropy, $x=0$, the Callen-Callen behavior is recovered. In the case of $\Delta J_{pq} = -0.2 \Delta J_{pq}^{\text{fit}}$, as in the $L1_0$ FePt and FePd systems,⁶ a nearly $K \propto m^2$ dependence over the whole temperature regime is obtained. Thus the remarkably different behavior of

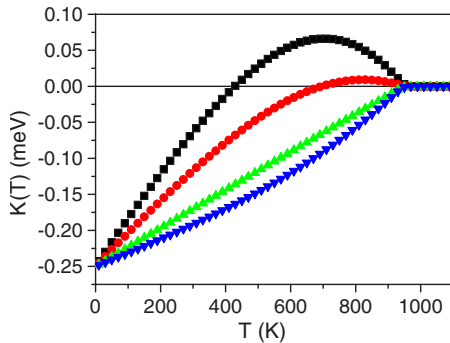


FIG. 5. (Color online) Magnetic anisotropy constant of the $\text{Co}_3/\text{Cu}(100)$ system vs temperature obtained from a mean-field approach of the Heisenberg model and scaling the exchange anisotropies $\Delta J_{pq} = x \Delta J_{pq}^{\text{fit}}$ with $\Delta J_{pq}^{\text{fit}}$ from Table II and the on-site anisotropies accordingly. Squares, $x=1$; circles, $x=0.5$; up triangles, $x=0.0$; down triangles, $x=-0.2$.

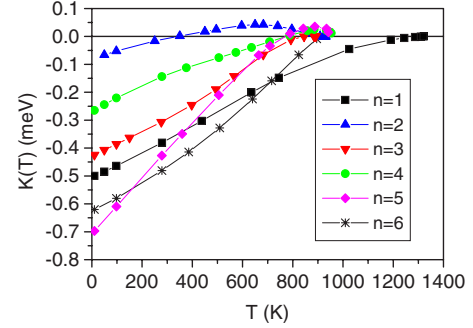


FIG. 6. (Color online) Calculated total magnetic anisotropy constant $K(T) = K_b(T) + K_{dd}(T)$ as a function of temperature for $\text{Co}_n/\text{Cu}(100)$.

$K(T)$ for different itinerant metallic magnets, i.e., $L1_0$ FePt and FePd vs $\text{Co}_n/\text{Cu}(100)$, can be interpreted as an effect of different magnitudes and, in particular, of different signs of the exchange anisotropies with respect to the corresponding on-site anisotropies.

As mentioned in Sec. II the total magnetic anisotropy energy is obtained by adding the magnetic dipole-dipole contribution [see Eq. (15)] to the band energy part $K_b(T)$. The corresponding results can be seen in Fig. 6. Since for layered systems $K_{dd}(T)$ is always negative, favoring thus an in-plane magnetization, except in the two-monolayer case, the total MA constants are shifted to negative values over almost the entire temperature range. Since, however, $K_{dd}(T)$ is proportional to $M(T)^2$, which goes to zero very rapidly at T_C , and since as shown above $K_b(T)$ exhibits a maximum, $K(T)$ slightly overshoots to positive values near T_C . This behavior is most pronounced for $n=2$, where $K(T) > 0$ between 350 K and T_C ($=933$ K).

Theoretically, such a temperature dependence of the MA constant implies a reorientation transition from an in-plane orientation to an out-of-plane orientation of the magnetization. However, as can be seen in Fig. 6 the positive values of $K(T)$ are very small and might be reduced by quite a few circumstances such as growth conditions, interface mixing, surface relaxations and stresses, or domain formation, which in turn make it difficult to relate this prediction to experiments. Indeed, so far such an inverse reorientation has not been found for Co films on Cu(001).

In conclusion we have presented a generalization of the recently introduced relativistic disordered local moments scheme^{5,6} to systems with two-dimensional translational symmetry. We also introduced recipes to calculate the Weiss fields and the magnetic anisotropy constants [see Eqs. (8) and (13)]. We implemented the RDLM method within the relativistic screened KKR code for layered systems and applied it to study the temperature dependence of the MAE of ferromagnetic Co films on Cu(001). Our results are in overall agreement with experiment as far as it is found that the magnetization is oriented parallel to the surface for almost all temperatures below the Curie temperature except for the two-monolayer system. Our calculations predict, however, also a reverse (in-plane to out-of-plane) spin reorientation

near T_C , which we interpreted in terms of a classical Heisenberg model and associated with relatively large exchange anisotropies arising due to itinerant electrons. As in the case of $\text{Co}_2/\text{Cu}(001)$, such a thermal reorientation effect seems to be most likely to occur for systems close to the reorientation at $T=0$, i.e., where $K(T=0)$ has a small negative value. Therefore, we expect that the *ab initio* RDLM scheme can describe well the temperature-induced reverse spin reorientation of 7–9 monolayer thick Ni films on $\text{Cu}(001)$ observed

experimentally²⁶ and studied theoretically in terms of a classical Heisenberg model.²⁷

ACKNOWLEDGMENTS

We acknowledge support by the Center for Computational Materials Science (Contracts No. FWF W004 and No. GZ 45.547) and by the Hungarian National Science Foundation (OKTA Grants No. T046267 and No. NF061726).

-
- ¹H. B. Callen and E. Callen, *J. Phys. Chem. Solids* **27**, 1271 (1966).
- ²A. Ecker, P. Fröbrich, P. J. Jensen, and P. J. Kuntz, *J. Phys.: Condens. Matter* **11**, 1557 (1999).
- ³S. Schwieger, J. Kienert, and W. Nolting, *Phys. Rev. B* **71**, 024428 (2005).
- ⁴O. N. Mryasov, U. Nowak, K. Y. Guslienko, and R. W. Chantrell, *Europhys. Lett.* **69**, 805 (2005).
- ⁵J. B. Staunton, S. Ostanin, S. S. A. Razee, B. L. Györfly, L. Szunyogh, B. Ginatempo, and E. Bruno, *Phys. Rev. Lett.* **93**, 257204 (2004).
- ⁶J. B. Staunton, L. Szunyogh, Á. Buruzs, B. L. Györfly, S. Ostanin, and L. Udvardi, *Phys. Rev. B* **74**, 144411 (2006).
- ⁷B. L. Györfly, A. J. Pindor, J. B. Staunton, G. M. Stocks, and H. Winter, *J. Phys. F: Met. Phys.* **15**, 1337 (1985).
- ⁸J. B. Staunton, B. L. Györfly, G. M. Stocks, and J. Wadsworth, *J. Phys. F: Met. Phys.* **16**, 1761 (1986).
- ⁹S. S. A. Razee, J. B. Staunton, L. Szunyogh, and B. L. Györfly, *Phys. Rev. B* **66**, 094415 (2002).
- ¹⁰J. Zabloudil, R. Hammerling, L. Szunyogh, and P. Weinberger, *Electron Scattering in Solid Matter*, Springer Series in Solid-State Sciences Vol. 147 (Springer, Heidelberg, 2005).
- ¹¹H. J. F. Jansen, *Phys. Rev. B* **59**, 4699 (1999).
- ¹²P. Lloyd, *Proc. Phys. Soc. London* **90**, 207 (1967); P. Lloyd and P. V. Smith, *Adv. Phys.* **21**, 69 (1972).
- ¹³X. D. Wang, R. Q. Wu, D. S. Wang, and A. J. Freeman, *Phys. Rev. B* **54**, 61 (1996).
- ¹⁴P. Weinberger and L. Szunyogh, *Comput. Mater. Sci.* **17**, 414 (2000).
- ¹⁵S. H. Vosko, L. Wilk, and M. Nusair, *Can. J. Phys.* **58**, 1200 (1980).
- ¹⁶B. Ginatempo and J. B. Staunton, *J. Phys. F: Met. Phys.* **18**, 1827 (1988).
- ¹⁷D. D. Johnson, *Phys. Rev. B* **38**, 12807 (1988).
- ¹⁸F. Huang, M. T. Kief, G. J. Mankey, and R. F. Willis, *Phys. Rev. B* **49**, 3962 (1994).
- ¹⁹G. J. Mankey, S. Z. Wu, F. O. Schumann, F. Huang, M. T. Kief, and R. F. Willis, *J. Vac. Sci. Technol. A* **13**(3), 1531 (1995).
- ²⁰L. Szunyogh and L. Udvardi, *J. Magn. Magn. Mater.* **198-199**, 537 (1999); L. Szunyogh and L. Udvardi, *Philos. Mag. B* **78**, 617 (1998).
- ²¹P. Bruno, *Phys. Rev. B* **43**, 6015 (1991).
- ²²M. Pajda, J. Kudrnovsky, I. Turek, V. Drchal, and P. Bruno, *Phys. Rev. Lett.* **85**, 5424 (2000).
- ²³P. J. Jensen and K. H. Bennemann, *Surf. Sci. Rep.* **61**, 129 (2006).
- ²⁴L. Szunyogh, B. Újfalussy, C. Blaas, U. Pustogowa, C. Sommers, and P. Weinberger, *Phys. Rev. B* **56**, 14036 (1997).
- ²⁵L. Udvardi, L. Szunyogh, A. Vernes, and P. Weinberger, *Philos. Mag. B* **81**, 613 (2001).
- ²⁶K. Baberschke and M. Farle, *J. Appl. Phys.* **81**, 5038 (1997).
- ²⁷A. Hucht and K. D. Usadel, *J. Magn. Magn. Mater.* **198**, 493 (1996).